Angewandte Chemie
Eine Zeitschrift der Gesellschaft Deutscher Chemiker

Supporting Information

for

Angew. Chem. Int. Ed. 200603651

$La_2MgNi_2H_8$, Containing Isolated $[Ni_2H_7]^{7-}$ and $[Ni_4H_{12}]^{12-}$ Anions

Jean-Noël Chotard, Yaroslav Filinchuk, Bernard Revaz and Klaus Yvon

Synthesis: Samples of nominal composition La_2MgNi_2 were synthesised in two steps. First, pellets of composition LaNi were prepared by mixing pieces of lanthanum with pressed powders of nickel and arc melted three times to assure good homogeneity. The LaNi ingots were then grinded in a glove box under argon atmosphere and mixed with magnesium powder. The resulting sample was pressed and placed into a tantalum tube which was sealed by an arc melting device in a glove box. The tube was placed in a resistance furnace and annealed under a vacuum of $3 \cdot 10^{-2}$ mbar during 2 hours at 400°C, and then during 2 hours at 600°C and 3 hours at 680°C. The tube was slowly cooled down to room temperature and opened in air. No oxidation was observed. The samples were single phase as found by XRD. Hydride and deuteride samples were prepared by activating the metal powder under vacuum ($3 \cdot 10^{-2}$ mbar) at 100°C overnight, and then charging with hydrogen (or deuterium) in autoclaves at 100°C and 30 bar pressure during 24 hours. Absorption was immediate as shown by the mass increase of the samples. The reaction products remained single phase as shown by XRD.

Synchrotron powder diffraction: A deuteride sample was studied by high-resolution synchrotron powder diffraction at the Swiss–Norwegian Beam Lines (BM01) at ESRF (Grenoble, France). It was filled into a thin-walled glass capillary of 0.4 mm diameter and measured in Debye–Scherrer geometry. Six Si (111) analyzers were used to record a diffraction pattern at $\lambda = 0.37504$ Å in the 2θ range 2.2–32.4° and with a step size of 0.004° (see supporting information). Absorption correction was applied by using the coefficient $\mu_r = 0.807$. Based on results of the automatic indexing program DICVOL04 [11] a new monoclinic cell was found and assigned to centrosymmetric space group $P2_1/c$. Structure refinement was carried out with the FULLPROF SUITE, starting with atomic coordinates as found by FOX [12] : 4 La, 4 Ni and 2 Mg sites, all on equipoint *4a* of space group $P2_1/c$. . Altogether, 57 parameters were refined: 1 scale factor, 6 background, 4 cell, 4 profile (pseudo-Voigt peak shape function) and 2 microstrain parameters to model anisotropic line broadening, 30 positional and 10 thermal parameters. Diffraction pattern and crystal data are given in Fig. 1 and Table 1 respectively.

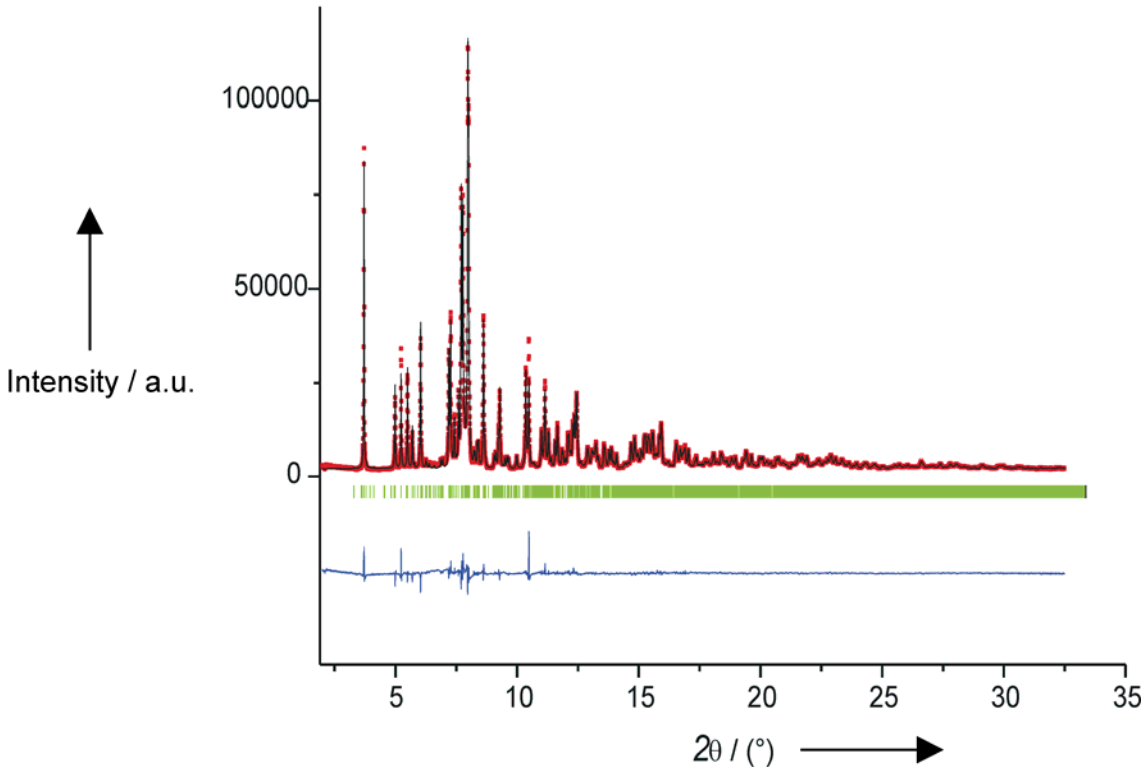

Figure 1 Synchrotron diffraction pattern of $La_2Ni_2MgD_8$ sample at room temperature (λ = 0.37504 Å)

Table 1: Atomic coordinates of $La_2Ni_2MgD_8$ as refined from synchrotron powder diffraction data. ($P2_1/c$, a=11.84482(1), b=7.821099(8), c= 11.96310(1) Å, β = 92.78 V=1106.96(2) Å^3, T=293 K, Rp = 0.069, Rwp = 0.081, χ^2=12.7). s.u. are listed in parenthesis.

Atom	Wyckoff position	x	y	z	B_{iso}
La1	4*a*	0.8324(2)	0.6605(4)	0.6817(2)	0.42(5)
La2	4*a*	0.6007(2)	0.6719(4)	0.4130(2)	0.64(5)
La3	4*a*	0.8971(2)	0.1561(4)	0.6115(2)	0.64(5)
La4	4*a*	0.6622(2)	0.3239(4)	0.8437(2)	0.48(5)
Ni1	4*a*	0.8513(4)	0.8524(7)	0.4567(3)	0.4(1)
Ni2	4*a*	0.3223(4)	0.643(1)	0.4203(4)	0.8(1)
Ni3	4*a*	0.0561(4)	0.6495(9)	0.1473(4)	1.0(1)
Ni4	4*a*	0.5696(4)	0.8730(9)	0.1798(4)	0.9(1)
Mg1	4*a*	0.902(1)	0.491(2)	0.4141(9)	0.3(2)
Mg2	4*a*	0.611(1)	0.501(3)	0.124(1)	1.6(3)

Neutron powder diffraction (NPD): Diffraction patterns (figure 2) were collected on a deuteride sample (mass ~6g) by using the high resolution powder diffractometer HRPT at SINQ (PSI, Villigen, Switzerland) in high intensity mode (λ = 1.8857 Å, 2θ range 5–164°, step size 0.1°, data collection time ~12 hours). Precise values of wavelengths were determined from measurements of a silicon standard. The deuterium atoms located by using FOX [12]. Sixteen deuterium positions on equipoint *4a* in space group $P2_1/c$ were located, corresponding to the composition $La_2MgNi_2D_8$. As their occupancy factors did not differ significantly from unity during preliminary structure refinements, they were fixed at this

value during subsequent refinement cycles. Atomic positions and inter-atomic distances of the two complex anions are given in Tables 2 and 3 respectively. The following 66 parameters were allowed to vary during structure refinement with the FULLPROF SUITE: 1 scale factors, 1 zero shift, 6 background, 48 positional and 4 thermal parameters, 4 profile (pseudo-Voigt peak shape function) and 2 microstrain parameters to model anisotropic line broadening. The refined diffraction pattern is given in Fig. 2, and a comparison between the metal positions in the deuteride and the intermetallic compound in Fig. 3.

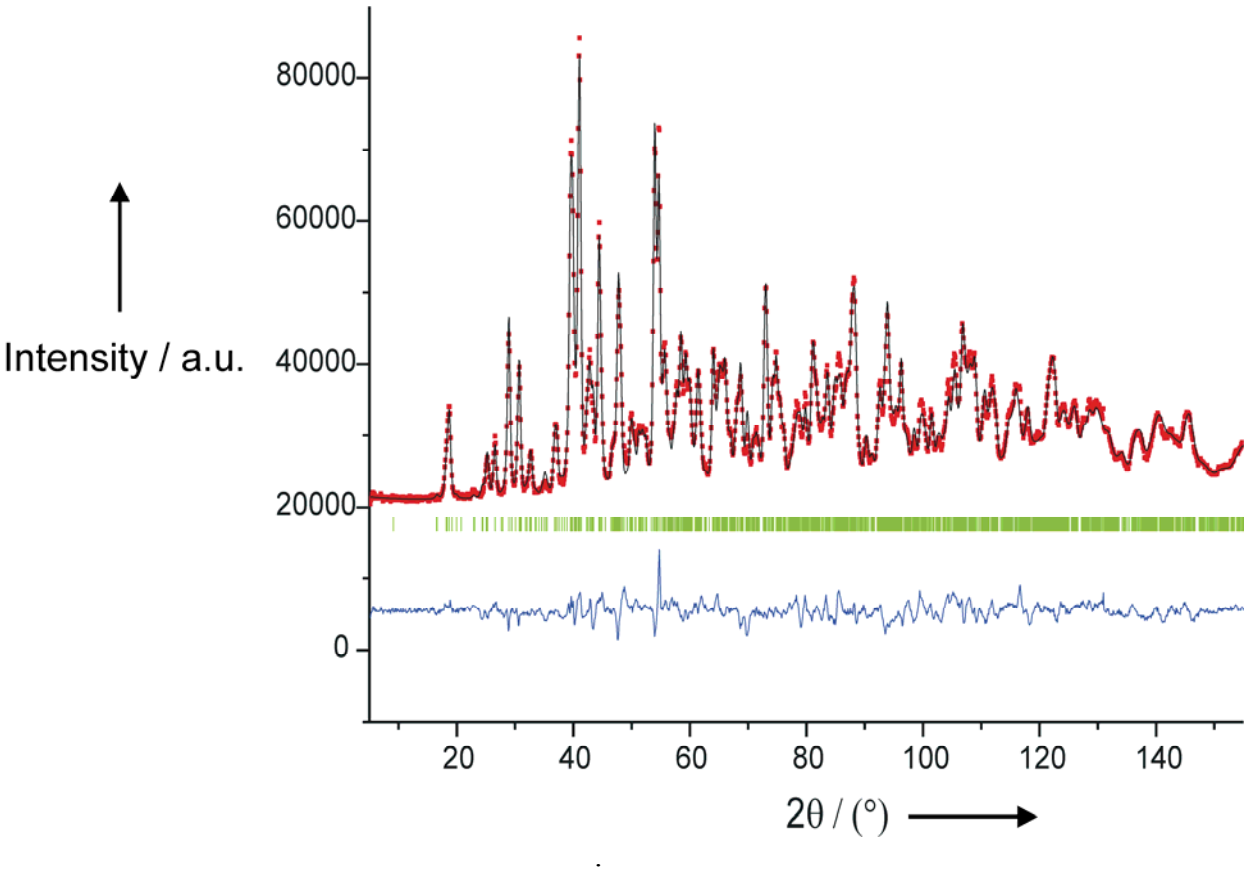

Figure 2 Neutron diffraction pattern of a $La_2MgNi_2D_8$ sample at room temperature (λ = 1.88577 Å)

Table 2 Atomic coordinates for $La_2Ni_2MgD_8$ as refined from NPD (λ=1.88577 Å). Space group: $P2_1/c$. Positions of metal atoms are fixed at the synchrotron values. Only deuterium atom positions are refined.

Atom	Wyckoff position	*x*	*y*	*z*	B_{iso}
La1	4*a*	0.8324(-)	0.6605(-)	0.6817(-)	0.30(6)
La2	4*a*	0.6007(-)	0.6719(-)	0.4130(-)	0.30(6)
La3	4a	0.8971(-)	0.1561(-)	0.6115(-)	0.30(6)
La4	4a	0.6622(-)	0.3239(-)	0.8437(-)	0.30(6)
Ni1	4*a*	0.85128(-)	0.85245(-)	0.45666(-)	1.21(6)
D11	4*a*	0.7444(14)	0.850(2)	0.5381(12)	2.43(6)
D12	4*a*	0.8460(13)	1.0489(19)	0.3997(14)	2.43(6)
D13	4*a*	0.9514(16)	0.8097(18)	0.5494(17)	2.43(6)
D14	4*a*	0.8282(15)	0.711(2)	0.3702(14)	2.43(6)
Ni2	4*a*	0.32226(-)	0.64273(-)	0.42029(-)	1.21(6)
D21	4*a*	0.4128(14)	0.797(2)	0.4490(15)	2.43(6)
D22	4*a*	0.2310(13)	0.628(2)	0.3208(15)	2.43(6)
D23	4*a*	0.4207(15)	0.506(3)	0.4137(16)	2.43(6)
D24	4*a*	0.2660(15)	0.579(3)	0.5288(15)	2.43(6)
Ni3	4*a*	0.05615(-)	0.64948(-)	0.14735(-)	1.21(6)
D31	4*a*	-0.0190(14)	0.579(2)	0.2381(16)	2.43(6)
D32	4*a*	0.0929(16)	0.819(2)	0.1952(14)	2.43(6)
Ni4	4*a*	0.56958(-)	0.87295(-)	0.17981(-)	1.21(6)
D41	4*a*	0.5434(16)	0.722(2)	0.1033(16)	2.43(6)
D42	4*a*	0.6700(15)	0.865(2)	0.2872(14)	2.43(6)
D43	4*a*	0.4516(15)	0.927(3)	0.2315(16)	2.43(6)
D1	4*a*	0.7538(18)	0.519(2)	0.2289(14)	2.43(6)
D2	4*a*	0.4296(14)	0.044(2)	0.5662(16)	2.43(6)
D3	4*a*	0.0602(15)	0.956(3)	0.9271(15)	2.43(6)
Mg1	4*a*	0.902(-)	0.491(-)	0.4141(-)	0.66(15)
Mg2	4*a*	0.611(-)	0.501(-)	0.124(-)	0.66(15)

Table 3 Nickel-deuterium distances in the two complex anions of $La_2Ni_2MgD_8$ as calculated from neutron diffraction data. s.u. are all equal or below 0.02 Å. (distances between the complexes are marked with a star)

Complex I		
Atom	Coordinated atoms	Distance (Å)
Ni2	D21	1.64
	D22	1.57
	D23	1.59
	D24	1.57
Ni4	D41	1.52
	D42	1.71
	D43	1.61
	D23	1.54

Complex II		
Atom	Coordinated atoms	Distances (Å)
Ni1	D11	1.64
	D12	1.68
	D13	1.62
	D14	1.53
	D42*	2.88*
Ni3	D31	1.54
	D32	1.50
	D12	1.53
	D13	1.70
	D22*	2.86*

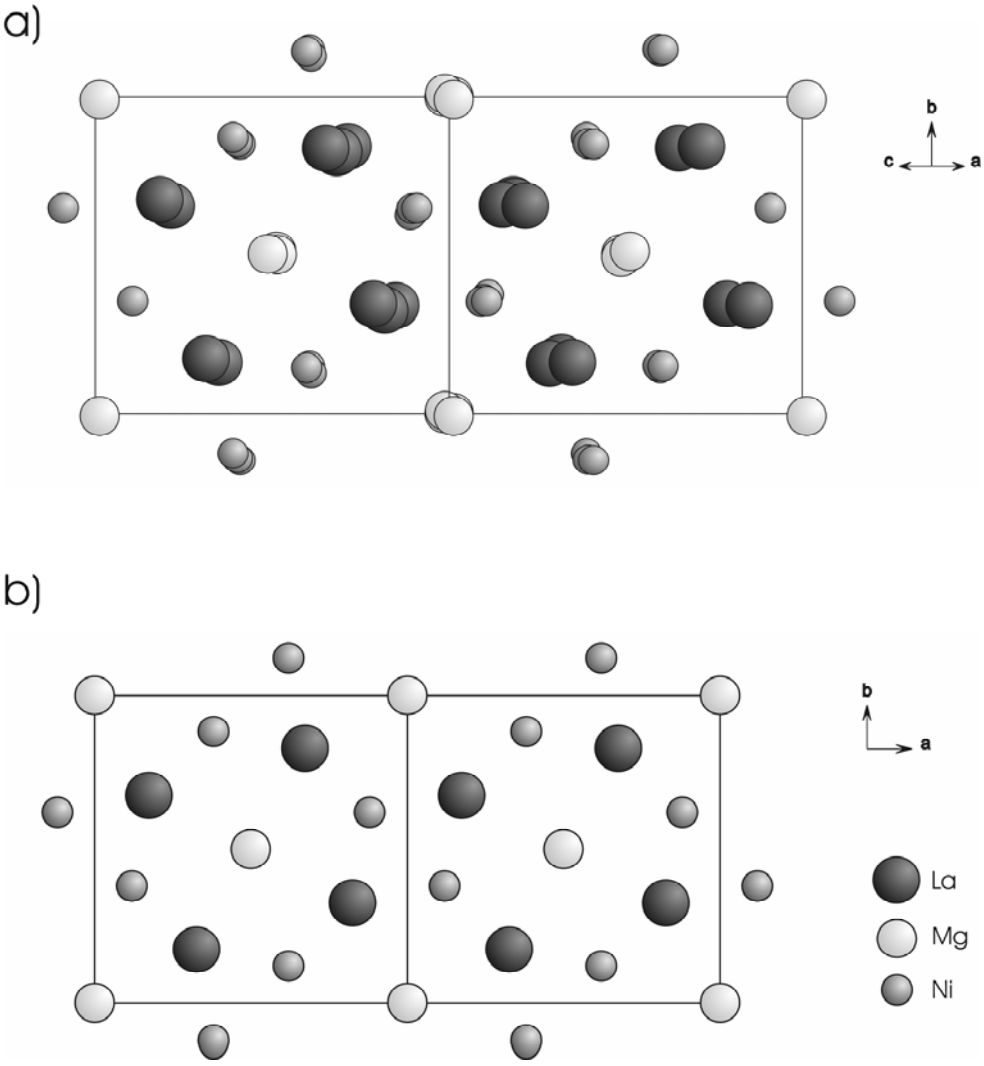

Figure 3: Comparison between the metal positions in a) the hydride (projection of one cell along monoclinic [101]) and b) the intermetallic compound (projection along tetragonal [001] of two cells). Deuterium atoms are omitted for clarity.

Electric resistance: Electric resistance measurements were performed by the four contact technique on a pressed powder of a hydride sample (parallelepiped of 10 × 4 × 1 mm^3). Voltage and current leads were attached by using silver paint. The pellet was mounted on an electrically insulator support, and then attached to the cold finger of a cryocooler. The range of dc current was 1×10^{-4} – 1×10^{-8} A. Data were recorded upon cooling during three consecutive runs from room temperature down to 10 K in steps of 5 K (Fig. 4). They showed an increase in resistivity consistent with non-metallic behaviour. Preliminary measurements on a piece of non hydrogenated sample showed a very small electric resistance consistent with metallic behaviour (~0.4 Ohm for a sample of 40mg).

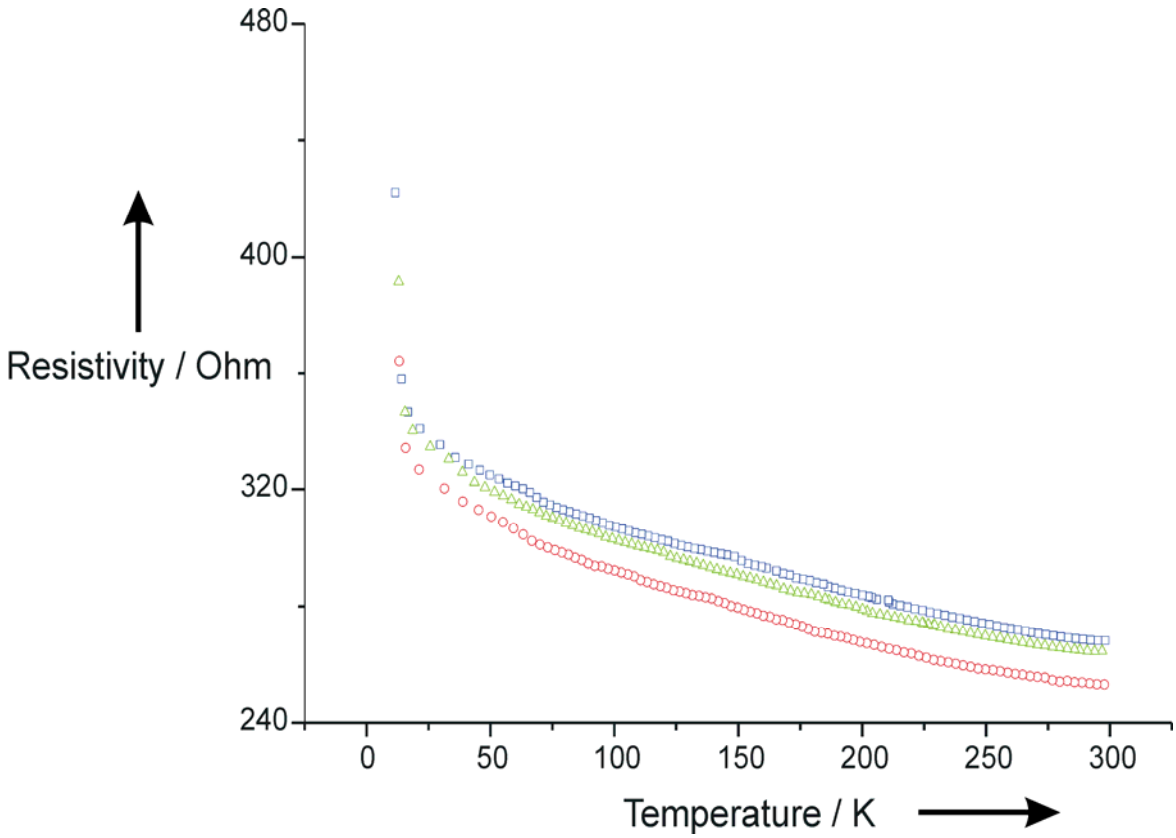

Figure 4: Electric resistance versus temperature curves of $La_2MgNi_2H_8$. Circles, triangles and squares represent respectively first, second and third cycle of measurements upon cooling.

Magnetism: Magnetization measurements have been performed using commercial MPMS SQUID magnetometer. Hysteresis measurements of the pure intermetallic La_2NiMg_2 sample (m=0.21773 g) and its hydride (m=0.2337 g), are presented in Figure 5 at three different temperatures (2, 10 and 50 K). To avoid extra ferromagnetic contaminations, new samples were prepared from very pure starting elements (Ni powder 99.999% from Sigma-Aldrich, Mg pieces 99.999% from Sigma-Aldrich, and high purity La from Ames Laboratory containing 5.22 ppm of Fe, 0.56 ppm of Ni and 0.09 ppm of Co). From the stated purities the total amount of iron and other metal impurities was estimated to be less than 27 ppm, i.e. much less than required to account for the ferromagnetic contribution. For both samples, the magnetisation data can be well fitted using two independent terms which are clearly seen in the raw data: a paramagnetic term M_para=χH and a constant ferromagnetic term M_ferro.

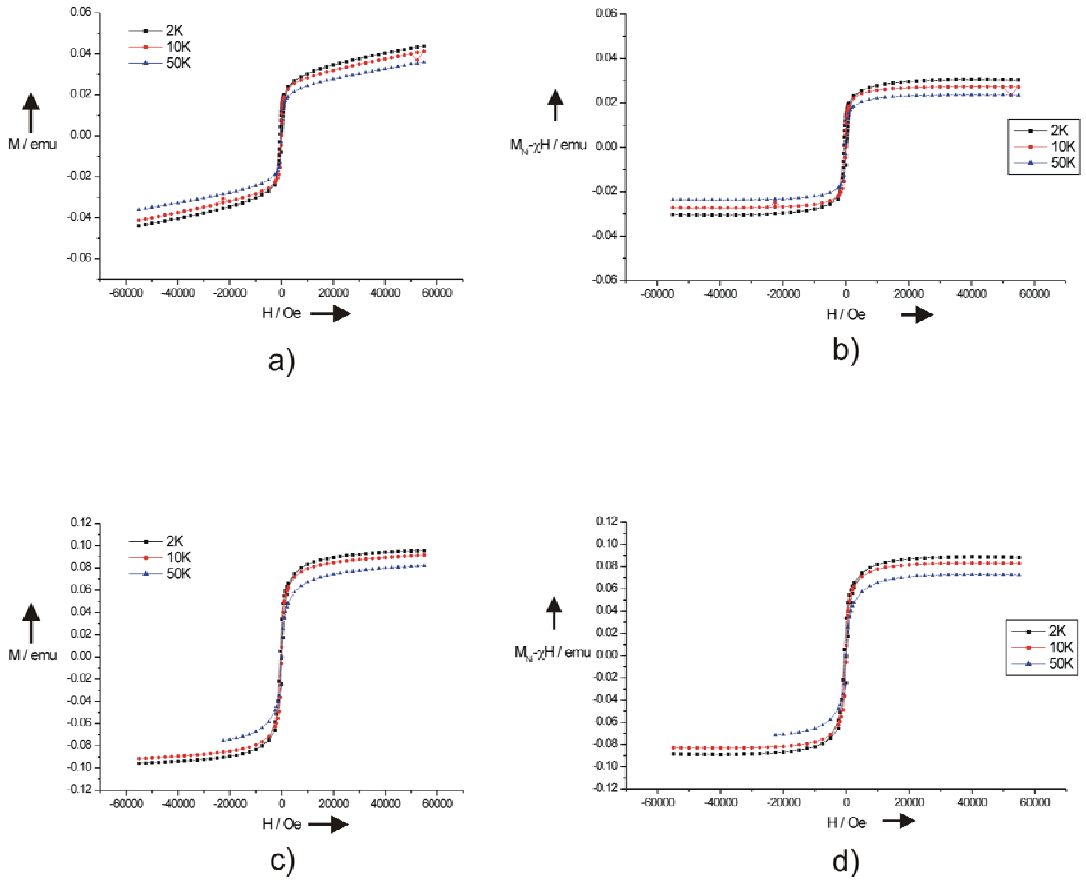

Figure 5: Magnetization curves of La_2MgNi_2 (a) and its hydride (c). Magnetization curves b) and d) show the ferromagnetic contribution of Ni in La_2MgNi_2 and $La_2MgNi_2H_8$, respectively.

These two terms are separated by assuming that, at the highest fields, typically above 25kOe, the magnetisation is the sum M=M_ferro + M_para, where M_para=χH is due to the paramagnetic response of the sample. The resulting values, fitted in the range 30-55kOe for each temperature, are given in Table 4.

Table 4: Fit of the magnetisation data for the intermetallic and hydride samples

T (K)	χ (emu/Oe)		M_ferro (emu)		χ (emu/Oe.g)	
	Intermetallic	Hydride	Intermetallic	Hydride	Intermetallic	Hydride
2	2.46E-07	1.32E-07	3.04E-02	8.86E-02	1.05E-06	6.08E-07
10	2.55E-07	1.58E-07	2.73E-02	8.30E-02	1.09E-06	7.26E-07
50	2.25E-07	1.72E-07	2.36E-02	7.28E-02	9.61E-07	7.88E-07

The contribution of the Ni phase has been estimated assuming bulk values (M_sat=54 emu/g). This gives an estimate of the quantity of segregated Ni, equivalent to 0.58mg and 1.67 mg in the La_2MgNi_2 and $La_2MgNi_2H_8$ samples respectively. Besides this ferromagnetic term, the alloy revealed a pronounced paramagnetic susceptibility ($1.05 \cdot 10^{-6}$ emu/g at 2 K), which is explained by a large electronic density of states at the Fermi energy, as seen in band structure calculations by Hoffmann (see ref [6] of main text). Upon hydrogenation, the paramagnetic susceptibility of the alloy is significantly decreased to $0.61 \cdot 10^{-6}$ emu/g (at 2 K). This behavior is consistent with the expected diamagnetism.